Electrochemistry and Spectroelectrochemistry of σ-Bonded Iron–Aryl Porphyrins. 2. Investigations of Six-Coordinate Complexes

D. Lançon,[1a] P. Cocolios,[1a] R. Guilard,[1b] and K. M. Kadish*[1a]

Department of Chemistry, University of Houston, Houston, Texas 77004, and Laboratoire de Synthèse et d'Electrosynthèse Organométallique Associé au CNRS (LA 33), Faculté des Sciences "Gabriel", 6, Bd Gabriel, 21100 Dijon, France

Received March 20, 1984

The electrochemistry, spectroelectrochemistry, and ^1H NMR spectroscopy of tetraphenyl and octaethyl six-coordinate σ-bonded iron–phenyl porphyrins were investigated in nonaqueous media. Formation constants for pyridine binding to (TPP)Fe(C_6H_5) and (OEP)Fe(C_6H_5) as well as the oxidized and reduced porphyrins were calculated in benzonitrile and ranged between $10^{3.5}$ and $10^{0.6}$ depending on the type of porphyrin ring and the overall charge of the porphyrin complex. Complexation of pyridine by the neutral (TPP)Fe(C_6H_5) or (OEP)Fe(C_6H_5) in C_5D_5N produced dramatic downfield shifts of the axial phenyl protons, suggesting that pyridine acts as a π acceptor when bonded to the low-spin iron(III) species. The oxidized and reduced six-coordinate species were also characterized by electronic absorption spectroscopy in pyridine and benzonitrile/pyridine mixtures and in both solvents suggested a nondiscrete site of reaction. Specifically, the product of the electrochemical oxidation could be described by a mixed formalism involving an Fe(IV) complex and an Fe(III) cation radical, while after reduction the spectra resembled both an Fe(II) complex and an Fe(III) anion radical.

Introduction

In part 1[2] of this series we reported electrochemical studies of (P)Fe(C_6H_5) (where P = OEP and TPP) in benzonitrile. At fast scan rates (>0.10 V/s) these compounds could be electroreduced to yield [(P)Fe(C_6H_5)]$^-$ or electrooxidized to yield [(P)Fe(C_6H_5)]$^+$. This latter species was not stable on the coulometric time scale of 1–15 min and chemically converted to [(N–C_6H_5P)Fe^{II}]$^+$ that was immediately oxidized to [(N–C_6H_5P)Fe^{III}]$^{2+}$. This electrochemically initiated iron to nitrogen migration of the phenyl group does not occur at fast scan rates or at low temperatures where reversible reactions are obtained. Under these conditions, the σ-bonded iron porphyrins undergo three reversible electron-transfer reactions as shown by eq 1–3.

$$(P)Fe(C_6H_5) + e \rightleftarrows [(P)Fe(C_6H_5)]^- \quad (1)$$

$$(P)Fe(C_6H_5) \rightleftarrows [(P)Fe(C_6H_5)]^+ + e \quad (2)$$

$$[(P)Fe(C_6H_5)]^+ \rightleftarrows [(P)Fe(C_6H_5)]^{2+} + e \quad (3)$$

The potentials for reaction 1 are among the most negative observed for reduction of five-coordinate iron(III) porphyrins. For the specific case of (TPP)Fe(C_6H_5) in benzonitrile, reduction occurs at $E_{1/2}$ = −0.70 V[2] which is a full 1.45 V from that for the corresponding Fe(III)/Fe(II) reaction of (TPP)Fe(NO).[3] Half-wave potentials for reaction 2 are also among the most negative observed for oxidation of five-coordinate iron(III) porphyrins. For the specific case of (TPP)Fe(C_6H_5) in benzonitrile, $E_{1/2}$ = +0.61 V.[2] This value is anodically shifted by 0.52 V from that reported for oxidation of (TPP)Fe(ClO_4) in the same solvent.[3]

The characterization and reactivity of five-coordinate σ-bonded iron porphyrins are well documented in the literature.[4-12] Nevertheless, very little is known regarding the chemistry and electrochemistry of six-coordinate σ-bonded iron porphyrin complexes. Thus, one aim of this paper is to characterize the potentials and stability of these type complexes.

In some cases,[13-16] addition of nitrogenous bases (such as pyridine) to five-coordinate iron porphyrins produces substantial changes in both the potentials and mechanisms of electrooxidation/reduction. For this reason, we have undertaken a study of oxidized, neutral, and reduced iron–phenyl porphyrins containing a bound pyridine ligand. Evidence for trans-axial coordination by pyridine is provided by ^1H NMR and spectrophotometric measurements (neutral species) as well as by electrochemical and spectroelectrochemical techniques (neutral, oxidized, and reduced complexes).

Experimental Section

Instrumentation. Electrochemical and spectroelectrochemical experiments were carried out on instrumentation described in

(1) (a) Department of Chemistry, University of Houston, Houston, TX 77004. (b) Laboratoire de Synthèse et d'Electrosynthèse Organométallique associé au CNRS (LA 33). Faculté des Sciences "Gabriel", 6, Bd Gabriel, 21100 Dijon, France.

(2) Lançon, D.; Cocolios, P.; Guilard, R.; Kadish, K. M. *J. Am. Chem. Soc.* **1984**, *106*, 4472–4478.

(3) Lançon, D.; Kadish, K. M. *J. Am. Chem. Soc.* **1983**, *105*, 5610.

(4) Mansuy, D.; Battioni, J.-P. *J. Chem. Soc., Chem. Commun.* **1982**, 638.

(5) Ortiz de Montellano, P. R.; Kunze, K. L.; Augusto, O. *J. Am. Chem. Soc.* **1982**, *104*, 3545.

(6) (a) Lexa, D.; Mispelter, J.; Saveant, J.-M. *J. Am. Chem. Soc.* **1981**, *103*, 6806. (b) Lexa, D.; Saveant, J.-M. *Ibid.* **1982**, *104*, 3503.

(7) Ogoshi, H.; Sugimoto, H.; Yoshida, Z. I.; Kobayashi, H.; Sakai, H.; Maeda, Y. *J. Organomet. Chem.* **1982**, *234*, 185.

(8) (a) Cocolios, P.; Laviron, E.; Guilard, R. *J. Organomet. Chem.* **1982**, *228*, C39. (b) Cocolios, P.; Lagrange, G.; Guilard, R. *Ibid.* **1983**, *253*, 65.

(9) Mansuy, D.; Battioni, J.-P.; Dupre, D.; Sartori, E. *J. Am. Chem. Soc.* **1982**, *104*, 6159.

(10) Battioni, P.; Mahy, J.-P.; Gillet, G.; Mansuy, D. *J. Am. Chem. Soc.* **1983**, *105*, 1399.

(11) Cocolios, P.; Lagrange, G.; Guilard, R.; Oumous, H.; Lecomte, C. *J. Chem. Soc., Dalton Trans.* **1984**, 567.

(12) Lagrange, G.; Cocolios, P.; Guilard, R. *J. Organomet. Chem.* **1984**, *260*, C16.

(13) Kadish, K. M.; Bottomley, L. A. *Inorg. Chem.* **1980**, *19*, 832.

(14) Walker, F. A.; Barry, J. A.; Balke, V. L.; McDermott, G. A.; Wu, M. Z.; Linde, P. F. *Adv. Chem. Ser.* **1981**, *No. 201*, 377.

(15) Kadish, K. M.; Bottomley, L. A.; Beroiz, D. *Inorg. Chem.* **1978**, *17*, 1124.

(16) Kadish, K. M. In "Iron Porphyrins", Part 2; Lever, A. B. P., Gray, H. B., Eds.; Addison-Wesley: Reading, MS, 1982; pp 161–249.

(17) Kadish, K. M.; Shiue, L. R. *Inorg. Chem.* **1982**, *21*, 1112.

0276-7333/84/2303-1164$01.50/0

Table I. ^{1}H NMR Chemical Shifts (δ) of (P)Fe(C_6H_5) in C_6D_6 and (P)Fe(C_6H_5)(py) in C_5D_5N at 294 K[c]

proton type	(OEP)Fe(C_6H_5)[a]		(OEP)Fe(C_6H_5)(py)		(TPP)Fe(C_6H_5)[a]		(TPP)Fe(C_6H_5)(py)	
porphyrin								
α-CH_2	m/8[b]	4.46	m/8	+0.07				
α'-CH_2	m/8	−1.70	m/8	−2.27				
β-CH_3	t/24	−1.76	s/24	−4.06				
meso	s/4	5.53	s/4	−3.23				
ortho phenyl					s/4	4.73	s/8	2.61
ortho′ phenyl					s/4	2.69		
meta phenyl					s/8	4.41	m/8	4.66
para phenyl					t/4	5.56	t/4	5.32
pyrrole					s/8	−17.64	s/8	−21.15
axial ligand								
o-H	s/2	−79.90	s/2	−55.70	s/2	−81.00	s/2	−55.00
m-H	s/2	13.23	s/2	16.30	s/2	13.55	s/2	18.85
p-H	s/1	−23.80	s/1	−8.90	s/1	−26.97	s/1	−11.67

[a] From ref 8. [b] s = singlet; t = triplet; m = multiplet. [c] Referenced to Me_4Si. Downfield shifts are given a positive sign.

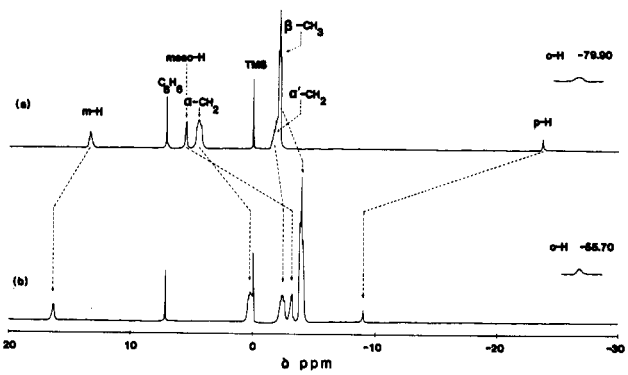

Figure 1. ^{1}H NMR traces of (OEP)Fe(C_6H_5) at 294 K in (a) C_6D_6 and (b) C_5D_5N.

a previous publication.[2] ^{1}H NMR spectra were recorded at 294 ● 1 K on a JEOL FT 100 spectrometer. Spectra were measured for argon-saturated solutions containing 6 mg of porphyrin in 0.5 mL of C_5D_5N (purchased from the "Commissariat à l'Energie Atomique (C.E.A.), France) using tetramethylsilane as internal reference.

Materials. (P)Fe(C_6H_5), where P = OEP and TPP, were synthesized from (P)FeCl and purified by column chromatography according to published procedures.[8] All solvents used for the electrochemical experiments were purchased as reagent grade quality. Benzonitrile (PhCN) was distilled from P_2O_5 under an inert atmosphere. Pyridine (py) was distilled from KOH and stored in the dark over activated 4-Å molecular sieves. The supporting electrolyte, tetra-*n*-butylammonium hexafluorophosphate (TBA(PF_6)), purchased from Fluka Co., was recrystallized from EtOH, dried in vacuo at 100 °C, and stored in a dessicator.

Results and Discussion

^{1}H NMR Measurements. The proton NMR traces of (OEP)Fe(C_6H_5) in C_6D_6 and C_5D_5N are shown in parts a and b of Figure 1 respectively. Table I summarizes the observed chemical shifts for the OEP and TPP derivatives in the above solvents. The spectra of (P)Fe(R) in noncoordinating solvents have been discussed extensively in an earlier paper[8] and the +III oxidation state of the iron and the $S = {}^1/_2$ spin state of the complex established. Analysis of the spectrum shown in Figure 1b and of the data listed in Table I suggests[18] that (OEP)Fe(C_6H_5) and (TPP)Fe(C_6H_5) are both low-spin iron(III) porphyrins in pyridine. However, although similar, their spectra exhibit marked differences. In particular, the separation between the signals of the diastereotopic α-CH_2 and α'-CH_2 protons of the OEP macrocycle is dramatically decreased when the solvent is pyridine ($\Delta\delta$ = 6.6 ppm in C_6D_6 and $\Delta\delta$ = 2.34 ppm in C_5D_5N). This difference in chemical shifts of the octaethyl porphyrin methylenic protons is directly related to the strength of the magnetic anisotropy between the two faces of the macrocycle and results from the position of the metal ion with respect to the porphyrin mean plane and the nature of its axial ligands.[19] The observed decrease in anisotropy when the spectrum is recorded in C_5D_5N is in accordance with trans coordination of iron by a pyridine molecule. Indeed such coordination must lead to displacement of the central iron toward the mean plane of the four nitrogen atoms of the macrocycle, thus reducing the magnetic nonequivalence of the CH_2 protons (Scheme I). The remaining anisotropy that is indicated by the 2.34 ppm separation of CH_2 signals may result from the difference in the nature of the two bound axial ligands, namely, phenyl and pyridine. This conclusion is strengthened by the unique broad resonance signal of the ortho phenyl protons of the TPP macrocycle observed in pyridine, as compared to the two distinct resonances at 4.73 and 2.69 ppm reported for the same protons in benzene (see Table I).

Scheme I

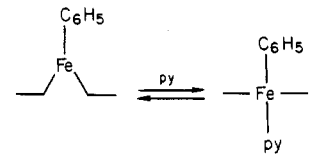

Chemical shifts for the protons of the axial phenyl group of (P)Fe(C_6H_4X) (X = H or CH_3) have been reported, and an M → L π charge transfer suggested on the basis of a sign change in the observed shifts (e.g., $\delta_{p\text{-}H}$ −23.80 for (OEP)Fe(C_6H_5) and $\delta_{p\text{-}CH_3}$ +60.10 for (OEP)Fe(p-$CH_3C_6H_4$)).[8] However, the hypothesis for delocalization of unpaired electron density on the lowest energy π* orbital of the aryl group cannot be totally eliminated, since the ortho phenyl resonance signals appear around −80 ppm.

Upon coordination by pyridine, the axial phenyl proton peaks of (TPP)Fe(C_6H_5) (Table I) shift downfield by 26.0, 5.30, and 15.30 ppm for the *o*-H, *m*-H, and *p*-H, respectively. Shifts of similar magnitude are also observed for the (OEP)Fe(C_6H_5) derivative. This pattern can be easily explained by assuming that pyridine acts as π acceptor when bonded to low-spin iron(III) complexes,[20] thus decreasing the magnitude of the M → L spin delocalization. This results in "polarization" of the Fe–C_6H_5 moiety

(18) La Mar, G. N.; Walker, F. A. In "The Porphyrins"; Dolphin, D., Ed.; Academic Press: New York, 1979; Vol. IV, Chapter 2.

(19) Busby, C. A.; Dolphin, D. *J. Magn. Reson.* **1976**, *23*, 211.

(20) Satterlee, J. D.; La Mar, G. N. *J. Am. Chem. Soc.* **1976**, *98*, 2804.

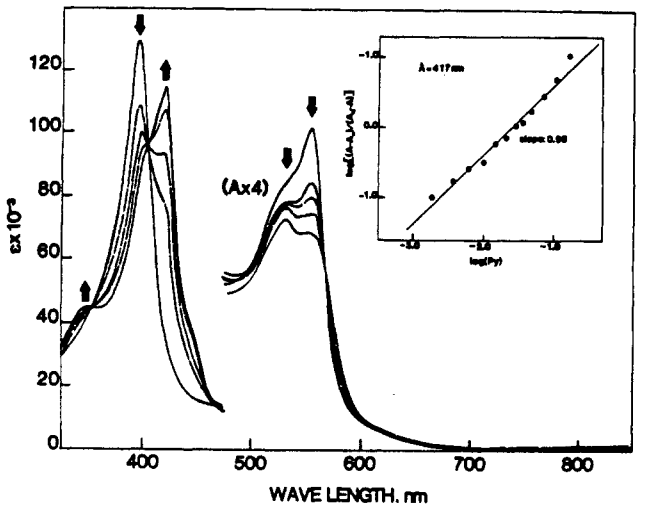

Figure 2. Spectral change observed during the titration of 1.50 × 10^{-5} M (OEP)Fe(C_6H_5) by py into PhCN, 0.1 M TBA(PF_6) solutions. Total concentration of py in solution: 0 M, 0.02 M, 0.074 M, 0.150 M, and 0.52 M.

leading to stabilization of the complex toward homolytic cleavage of the iron–carbon σ bond.[7]

Spectrophotometric Titration. Complexation of one pyridine molecule to the neutral (P)Fe(C_6H_5) complex is represented by eq 4.

$$(P)Fe(C_6H_5) + py \overset{\beta_1^0}{\rightleftharpoons} (P)Fe(C_6H_5)(py) \qquad (4)$$

Spectral changes obtained upon addition of pyridine to (OEP)Fe(C_6H_5) in benzonitrile solutions are shown in Figure 2. Analysis of the spectral data by plotting log $[(A - A_\infty)/(A_0 - A)]$ vs. log [py] resulted in a linear relationship with a slope of 1.0, indicating the addition of one py molecule to the starting species. The formation constant of (OEP)Fe(C_6H_5)(py) was calculated as log $\beta_1^0 = 1.6 \pm 0.1$ for reaction 4. Furthermore, clear isosbestic points reveal only the five- and six-coordinate species in equilibrium.

Formation of (OEP)Fe(C_6H_5)(py) results in a red shift of the Soret band (from 393 to 417 nm) together with the appearance of three shoulders and α and β bands characterizing a metal → ligand charge transfer common in iron(II) porphyrins. This is not surprising since the electron density on the iron center might be increased by the inductive effect of the axial ligand(s).

Electrode Reactions in py/PhCN Mixtures. The electrochemistry of (OEP)Fe(C_6H_5) and (TPP)Fe(C_6H_5) is similar in py/PhCN mixtures as that observed in neat PhCN. This is shown in Figure 3 for the case of (TPP)-Fe(C_6H_5). In neat PhCN a reversible reduction (reaction 1) occurs at −0.70 V while two oxidations are observed at +0.61 and +1.49 V (reactions 2 and 3). When pyridine is added to PhCN solutions of (TPP)Fe(C_6H_5), reaction 3 becomes obscured by the oxidation of pyridine. However, both the first reduction (labeled reaction I in Figure 3) and the first oxidation (labeled reaction II in Figure 3) shift negatively from the values reported in PhCN while the reversibility of the reaction is maintained. The magnitudes of the potential shifts are not equal for the two reactions, and values of $E_{1/2}$ are dependent on the free pyridine concentration in solution.

At [py] < 10^{-2} M (not shown in Figure 3), $E_{1/2}$ for reaction II shifts negatively by 50 mV per tenfold change in [py] while the half-wave potential for reaction I remains constant at $E_{1/2} = -0.70$ V. This dependence of $E_{1/2}$ on [py] is consistent with a five-coordinate (TPP)Fe(C_6H_5) species at low pyridine concentration but suggests that a

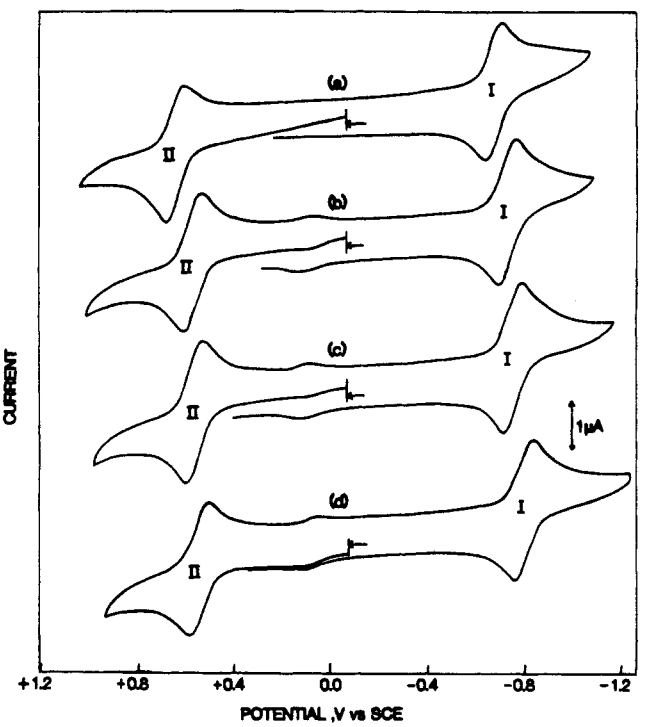

Figure 3. Cyclic voltammograms of 7.79 × 10^{-4} M (TPP)Fe(C_6H_5) in mixed py/PhCN solvents containing 0.1 M TBA(PF_6) (scan rate = 0.10 V/s). Pyridine concentrations: (a) 0 M; (b) 0.062 M; (c) 0.160 M; (d) 2.9 M.

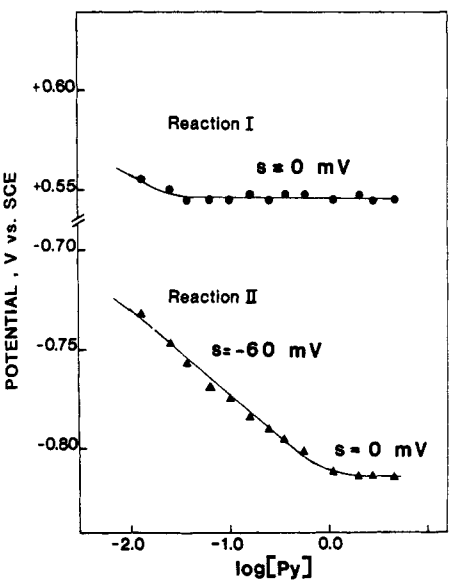

Figure 4. Plot of the first oxidation and first reduction half-wave potentials of 7.79 × 10^{-4} M (TPP)Fe(C_6H_5) versus log [py] during the titration presented in Figure 3.

pyridine is bound to the first oxidation product as shown in eq 5. The theoretical shift of $E_{1/2}$ with log [py] is −58

$$(TPP)Fe(C_6H_5) + py \rightleftarrows [TPP)Fe(C_6H_5)(py)]^+ + e \qquad (5)$$

mV for such a reaction,[21] and this agrees well with the experimental value of −50 mV. In addition, confirmation that the neutral complex was not ligated also comes from the electronic absorption spectra that are identical in

(21) Laitenen, H. A.; Harris, W. E., "Chemical Analysis"; McGraw-Hill: New York, 1975; pp 227–231.
(22) Nicholson, R. S.; Shain, I. *Anal. Chem.* 1964, *36*, 706.
(23) Kadish, K. M.; Bottomley, L. A.; Kelly, S.; Schaeper, D.; Shiue, L. R. *Bioelectrochem. Bioenerg.* 1981, *8*, 213.

Scheme II

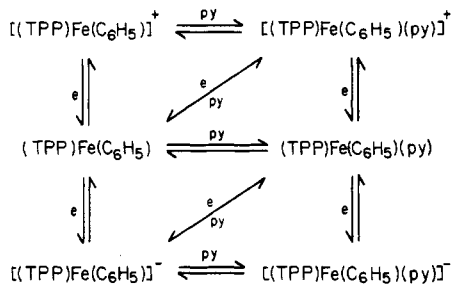

PhCN and in PhCN containing less than 10^{-2} M py.

Shifts of $E_{1/2}$ upon larger additions of pyridine are shown in parts b–d of Figure 3, and values of $E_{1/2}$ vs. log [py] are plotted in Figure 4. Between [py] = 0.016 M and [py] = 1.0 M the first oxidation potential remains constant at $E_{1/2}$ = +0.53 V while the first reduction is shifted by −60 mV per log [py]. Similar plots have been presented for the oxidation/reduction of (TPP)Fe(Cl) in the presence of nitrogenous bases[13-16] and, for the specific case of (TPP)-Fe(C_6H_5), suggest the electrode reactions shown in eq 6 and 7.

$$(TPP)Fe(C_6H_5)(py) \rightleftarrows [(TPP)Fe(C_6H_5)(py)]^+ + e \quad (6)$$

$$(TPP)Fe(C_6H_5)(py) + e \rightleftarrows [(TPP)Fe(C_6H_5)]^- + py \quad (7)$$

Finally, at [py] > 1.0 M both the oxidation and the reduction potentials are independent of [py], indicating complexation of a pyridine molecule by the neutral, oxidized, and reduced forms of the complex. Under these experimental conditions the oxidation is given by eq 6 while the reduction can be represented by eq 8.

$$(TPP)Fe(C_6H_5)(py) + e \rightleftarrows [(TPP)Fe(C_6H_5)(py)]^- \quad (8)$$

Combinations of reactions 1 and 2 in PhCN with reactions 5–8 in py/PhCN mixtures leads to the overall oxidation/reduction mechanism shown in Scheme II for the case of the TPP derivative.

Experiments carried out on (OEP)Fe(C_6H_5) in mixed py/PhCN solutions lead to potential shifts similar to those shown in Figure 4 and to a mechanism almost identical with that illustrated in Scheme II. However, pyridine appears to coordinate less strongly to the neutral (OEP)Fe(C_6H_5) than to the neutral (TPP)Fe(C_6H_5). This conclusion is based on the fact that shifts in reduction potential of (OEP)Fe(C_6H_5) do not occur until [py] > 0.3 M. In addition, [(OEP)Fe(C_6H_5)(py)]$^-$ is not observed at any ligand concentrations up to 5.0 M py, suggesting a very low py binding constant for [(OEP)Fe(C_6H_5)]$^-$.

Formation Constants for Pyridine Binding. Complexation of one pyridine molecule to the neutral, oxidized, and reduced forms of (P)Fe(C_6H_5) is represented by eq 4, 9, and 10, respectively. Values of β_1^0 were calculated

$$[(P)Fe(C_6H_5)]^+ + py \overset{\beta_1^+}{\rightleftarrows} [(P)Fe(C_6H_5)(py)]^+ \quad (9)$$

$$[(P)Fe(C_6H_5)]^- + py \overset{\beta_1^-}{\rightleftarrows} [(P)Fe(C_6H_5)(py)]^- \quad (10)$$

directly from spectrophotometric titrations, while β_1^+, β_1^-, and also β_1^0 are easily determined from shifts of $E_{1/2}$ as a function of ligand concentration. This latter method of calculation has been described in the literature[13-17] and utilizes the type of data illustrated in Figure 4.

Reaction 4 was also monitored by evaluating shifts in reduction potential as a function of log [py]. Values of log β_1^0 were 1.8 ± 0.2 for (OEP)Fe(C_6H_5) and 2.5 ± 0.2 for (TPP)Fe(C_6H_5). In the former case, the electrochemical value is within experimental error of that calculated by the spectrophotometric titration (log β_1^0 = 1.6 ± 0.1). Values of log β_1^0 were then utilized to calculate log β_1^+ and log β_1^-. These values are presented in Table II that summarizes all of the measured formation constants for pyridine addition. As seen in this table, the ligation ability of the σ-bonded iron complexes decreases along the sequence cation > neutral > anion. A similar trend has been observed for the formation of oxidized and reduced (TPP)-Zn(py) complexes[17] and is not unexpected.

Table II. Formation Constants[a] for the Addition of py to [(P)Fe(C_6H_5)]$^+$, (P)Fe(C_6H_5), and [(P)Fe(C_6H_5)]$^-$

porphyrin	log β_1^+	log β_1^0	log β_1^-
(OEP)Fe(C_6H_5)	3.5 ± 0.2	1.6 ± 0.1[b] 1.8 ± 0.2	NR
(TPP)Fe(C_6H_5)	3.9 ± 0.3	2.5 ± 0.2	0.6 ± 0.2

[a] Unless indicated all values were calculated from electrochemical titration data. [b] Calculated from spectrophotometric titration data. NR = no reaction.

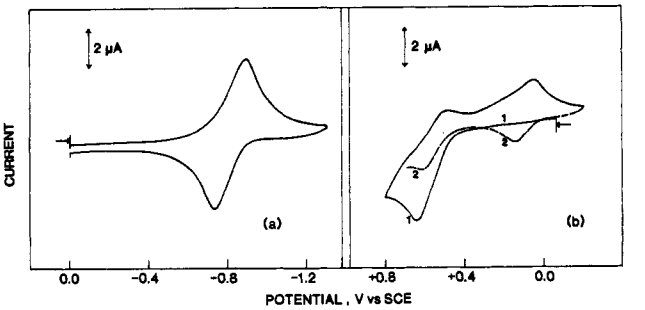

Figure 5. Thin-layer cyclic voltammogram of 5.8 × 10^{-4} M (TPP)Fe(C_6H_5) in PhCN, 0.3 M TBA(PF_6) (scan rate = 0.002 V/s): (a) first reductive scan; (b) first and second oxidative scan.

Reduction of (P)Fe(C_6H_5)(py) in py/PhCN Mixtures. The reduction of (P)Fe(C_6H_5)(py) is reversible at the OTTLE time scale for all concentrations of pyridine. This is shown by the cyclic voltammogram in Figure 5a and the corresponding OTTLE spectra in Figure 6. (OEP)Fe(C_6H_5)(py) is generated from (OEP)Fe(C_6H_5) at [py] > 0.3 M, and, at all concentrations of pyridine, this species is reduced to [(OEP)Fe(C_6H_5)]$^-$.

The dissociation of a py ligand is also observed upon reduction of (TPP)Fe(C_6H_5)(py) at [py] < 1.74 M. At higher concentrations of pyridine, however, reduction of (TPP)Fe(C_6H_5)(py) yields [(TPP)Fe(C_6H_5)(py)]$^-$ as shown in eq 8 and illustrated in Figure 6b. As seen in this figure, the optical spectrum of the reduced species is quite different from that for [(TPP)Fe(C_6H_5)]$^-$ (see Table III). The Soret and Q bands of the obtained complex are red shifted (Δλ = 22 and 21 nm, respectively) when compared to the bands of [(TPP)Fe(C_6H_5)]$^-$ and suggest axial coordination of the anion by pyridine. In addition, a well-defined absorption maximum at 768 nm suggests the presence of a radical anion. Consequently, the reduction process involves two resonance contributors as shown in eq 11. Reaction 11 is similar to that reported for the

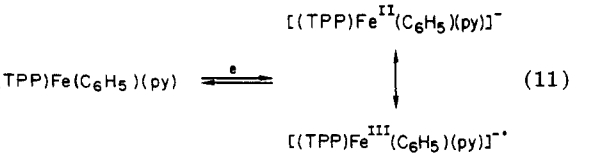

(11)

reduction of [(P)Fe(C_6H_5)] in PhCN.[2] However, in py/PhCN mixtures the molar absorptivity of the band attributed to a radical anion is weaker than the one observed in PhCN, suggesting a less important contribution of the radical character to the six-coordinate reduced complex.

Table III. Spectral Data for Five- and Six-Coordinate (P)Fe(C_6H_5) Complexes[a]

ring	species	λ_{max}, nm ($10^{-3}\epsilon$)	
OEP	[(OEP)Fe(C_6H_5)]$^+$ [b]	392 (120)	530 (20), 555 (sh)
	[(OEP)Fe(C_6H_5)(py)]$^+$	367 (sh), 400 (118)	512 (19), 539 (17), 752 (3)
	(OEP)Fe(C_6H_5) [b]	393 (129)	527 (sh), 554 (22)
	(OEP)Fe(C_6H_5)(py)	360 (sh), 405 (sh), 417 (115)	531 (16), 554 (15)
	[(OEP)Fe(C_6H_5)]$^-$ [b]	350 (42), 408 (98)	502 (19), 542 (57), 758 (7)
TPP	(TPP)Fe(C_6H_5) [b]	398 (sh), 412 (93)	522 (12), 541 (sh)
	(TPP)Fe(C_6H_5)(py)	357 (sh), 408 (sh), 431 (92)	532 (9), 631 (2)
	[(TPP)Fe(C_6H_5)]$^-$ [b]	364 (36), 429 (98)	510 (14), 533 (sh), 571 (4), 765 (4)
	[(TPP)Fe(C_6H_5)(py)]$^-$	366 (30), 432 (55), 451 (74)	531 (14), 552 (sh), 768 (2)

[a] In py/PhCN, 0.1 M TBA(PF_6). [b] Taken from ref 2.

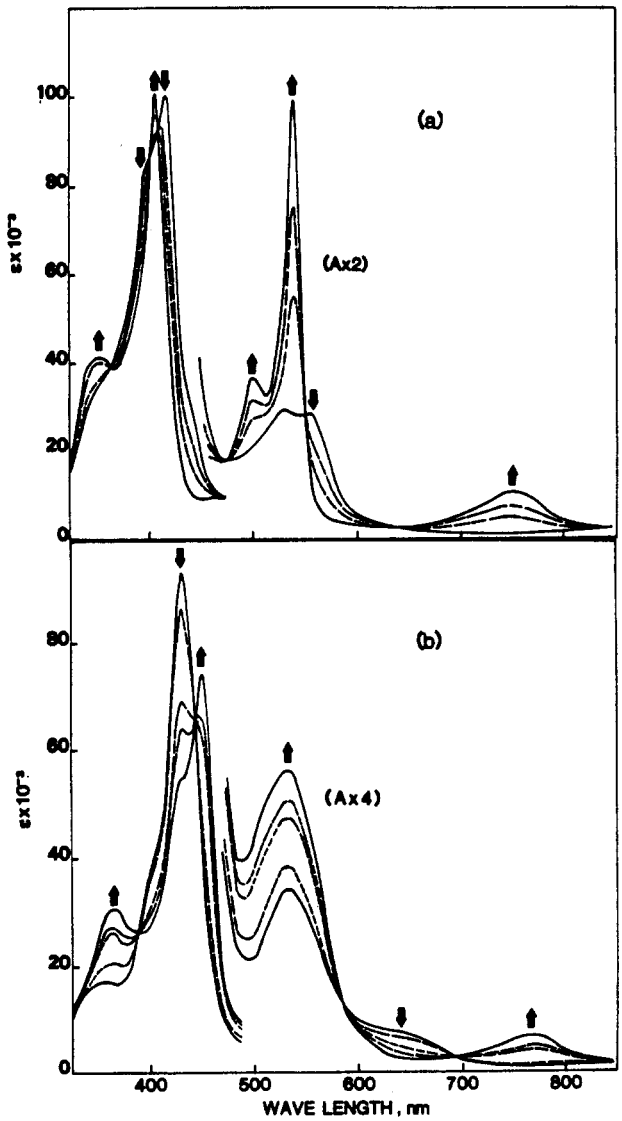

Figure 6. Time-resolved electronic absorption spectra taken at an OTTLE during the reduction of (a) 6.0×10^{-4} M (OEP)Fe(C_6H_5)(py) at 0, 5, 25, and 300 s of electrolysis and (b) 5.8×10^{-4} M (TPP)Fe(C_6H_5)(py), in py/PhCN, 0.3 M TBA(PF_6) solutions at 0, 5, 20, 60 and 240 s of electrolysis. In both cases [py]/[porphyrin] = 2000.

The formation of [(TPP)Fe^{III}(C_6H_5)(py)]$^-$· in parallel with that of [(TPP)Fe^{II}(C_6H_5)(py)]$^-$ may be compared to the change in oxidation site of some iron(II) tetrapyrrolic complexes upon coordination by carbon monoxide. Indeed, it has been shown that both (EtioC)Fe^{II}(CO)(py)[24] and (TBP)Fe^{II}(CO)(py)[25] may be oxidized to yield the corresponding Fe(II) cation radical rather than an Fe(III) species (where EtioC = etiochlorin I and TBP = tetrabenzoporphyrin). Vogler et al.[25] have pointed out that formation of an Fe(II) cation radical results from negatively shifting the half-wave potential for π cation radical formation such that this reaction preferentially occurs over an electrode reaction producing Fe(III). Presumably a similar negative shift occurs for the Fe(III) $\rightleftarrows$ Fe(II) reaction of (TPP)Fe(C_6H_5)(py) such that the potentials for Fe(III) π anion radical formation and that for Fe(II) formation are closely overlapped. This thus produces what appears to be the first example of an Fe(III) anion radical (as depicted by eq 11 above).

Oxidation of (P)Fe(C_6H_5)(py) in py/PhCN Mixtures. (TPP)Fe(C_6H_5)(py) and (OEP)Fe(C_6H_5)(py) were oxidized at an OTTLE with monitoring of the electrogenerated products. At the OTTLE time scale (P)Fe(C_6H_5)(py) behaves like the corresponding five-coordinate complexes in benzonitrile,[2] giving rise to a slow chemical reaction (see Figure 5b) leading to [(N–C_6H_5P)Fe^{III}]$^{2+}$. This species is reversibly reduced at +0.10 V (TPP) or −0.16 V (OEP). Time-resolved spectra during the oxidation of (OEP)Fe(C_6H_5)(py) (see Figure 7a) show, however, the initial formation of a cationic species with blue-shifted Q bands and molecular absorptivities similar to those of the neutral (OEP)Fe(C_6H_5)(py) complex (see Table III). Furthermore, a weak and broad absorption centered at 752 nm appears in the spectrum. These features are consistent with a partially metal-centered and a partially ring-centered oxidation, the main contributor being an iron(IV) form as depicted in eq 12.

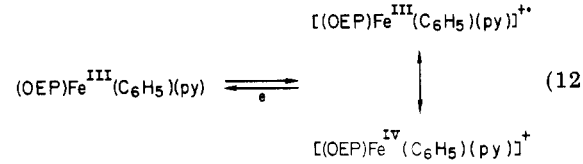

(12)

Upon reduction of [(N–C_6H_5P)Fe^{II}]$^+$ a nitrogen to iron back-migration also occurs at low pyridine concentrations. This electrochemically initiated reaction involves a two-electron transfer and takes place at [py] < 0.13 M for P = TPP and [py] < 0.3 M for P = OEP. At higher concentrations of pyridine, cleavage of the phenyl group occurs and (TPP)Fe(py)$_2$ or (OEP)Fe(py)$_2$ is formed. The scheme of the total reversible iron to nitrogen migration of the phenyl group is shown in Figure 8 for the (OEP)Fe(C_6H_5) derivative in pyridine. An identical mechanism is observed for (TPP)Fe(C_6H_5) with the exception that the obtained anion is hexacoordinated (see eq 11).

Electrochemistry in Neat Pyridine. In pyridine, 0.1 M TBA(PF_6), both (OEP)Fe(C_6H_5) and (TPP)Fe(C_6H_5) exhibit a single quasi-reversible reduction and a single quasi-reversible oxidation (see Table IV). In addition, a second irreversible oxidation is observed for the OEP derivative at E_{pa} = +1.29 V. The peak current ratio i_{pc}/i_{pa}

(24) Chang, C. K.; Fajer, J. *J. Am. Chem. Soc.* **1980**, *102*, 848.
(25) Vogler, A.; Rethwisch, B.; Kunkely, H.; Hüttermann, J. *Angew. Chem., Int. Ed. Engl.* **1978**, *17*, 952.

Table IV. Half-wave Potentials for Oxidation and Reduction of (P)Fe(C_6H_5) in py and PhCN Containing 0.1 M TBA(PF_6)

compd	solv	$E_{1/2}$, V vs. SCE: 2nd oxidatn	1st oxidatn	1st reductn	$E_{1/2}$(Fc^+/Fc)
(OEP)Fe(C_6H_5)	py	+1.29[a]	+0.44	−1.03	+0.52
	PhCN[b]	+1.30	+0.48	−0.93	+0.46
(TPP)Fe(C_6H_5)	py		+0.63	−0.76	+0.52
	PhCN[b]	+1.49[a]	+0.61	−0.70	+0.46

[a] Potential quoted is E_{pa} measured at 0.10 V/s. [b] Taken from ref 2.

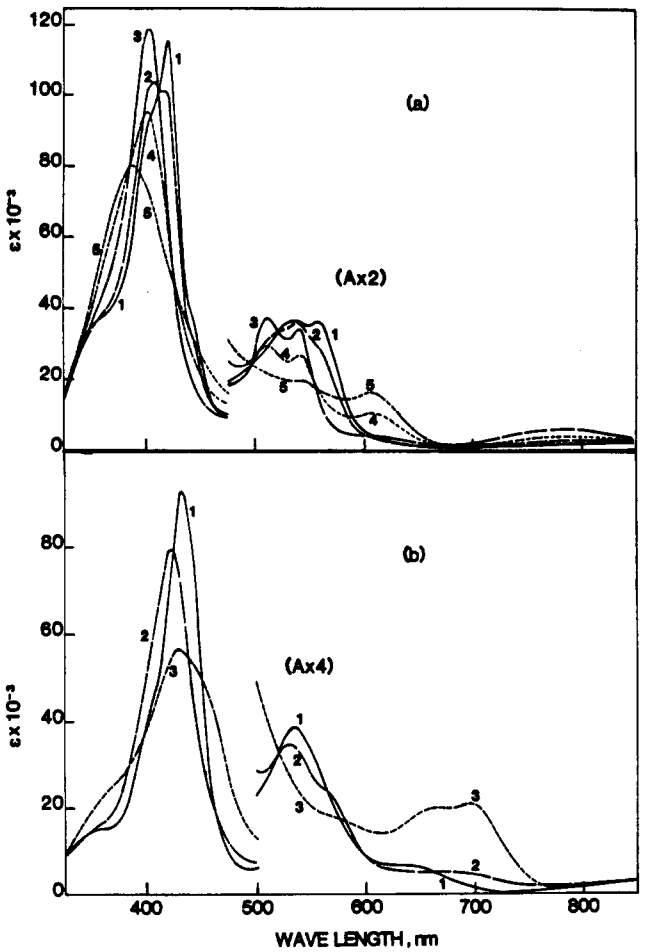

Figure 7. Time-resolved electronic absorption spectra taken at an OTTLE during the oxidation of (a) 6.0 × 10^{-4} M (OEP)Fe(C_6H_5)(py) at a [py]/[porphyrin] ratio of 510 (total electrolysis times, (1) 0 s, (2) 15 s, (3) 45 s, (4) 300 s, and (5) 1200 s) and (b) 6.7 × 10^{-4} M (TPP)Fe(C_6H_5)(py) in py/PhCN, 0.3 M TBA(PF_6) at a [py]/[porphyrin] ratio of 150 (total electrolysis times, (1) 0 s, (2) 30 s, and (3) 780 s.

for the first oxidation is close to 1.0 at scan rates above 0.05 V/s while i_{pa}/i_{pc} for the single reduction ranges between 0.75 and 1.0 and increases with scan rate. The data for the latter case are in accordance with a slow chemical reaction following electron addition.[22] This EC mechanism was confirmed by the appearance of a reversible wave upon reoxidation. Half-wave potentials for this wave were at $E_{1/2}$ = −0.15 for P = OEP and $E_{1/2}$ = +0.06 V for P = TPP. These potentials match those reported[13,23] for [(OEP)Fe(py)$_2$]$^+$ and [(TPP)Fe(py)$_2$]$^+$ and indicate partial displacement of the axial phenyl group by a pyridine molecule as shown in eq 13.

$$(P)Fe(C_6H_5)(py) + py \rightleftarrows (P)Fe(py)_2 \qquad (13)$$

Effect of the Sixth Pyridine Ligand and Site of the Electrode Reactions. As shown in this work, pyridine coordinates to the iron center of (P)Fe(C_6H_5). Moreover, reductive elimination of the phenyl group and formation

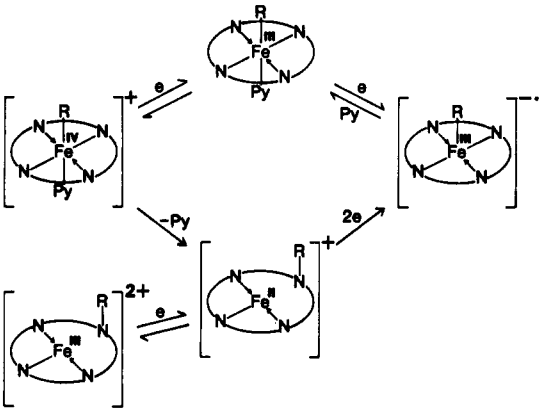

Figure 8. Reversible iron to nitrogen migration for (OEP)Fe(C_6H_5)(py) in py/PhCN mixtures.

of the bis-pyridine adduct of iron(II) can also take place. This reaction has already been reported for other iron(II)–alkyl organometallic complexes[26] and, in the case of (P)Fe(R) porphyrins, is accelerated upon one-electron reduction.

A comparison of log β_1 values obtained for the oxidized, neutral, and reduced complexes indicates that the ligation ability of the σ-bonded iron complexes decreases along the sequence cation > neutral > anion. Consequently, pyridine addition stabilizes the neutral and oxidized species and lowers the chemical reactivity of these complexes. This has been proven by a slower metal to nitrogen migration for [(P)Fe(C_6H_5)(py)]$^+$ than for [(P)Fe(C_6H_5)]$^+$. Furthermore, the relative stabilization of the neutral species upon addition of one pyridine molecule is in accordance with a decrease in the metal to ligand spin delocalization. This is also indicated by the ^{1}H NMR measurements.

The one electron reduction of (P)Fe(C_6H_5)(py) yields a six-coordinate (P = TPP) or a five-coordinate (P = OEP) species that can be described by a mixed iron(III) radical anion and iron(II) porphyrin formalism. This is similar to a postulated formalism for reduced [(P)Fe(C_6H_5)]$^-$ in nonbonding media.[2] However, the molar absorptivity of the absorption band at 765–768 nm that characterizes a radical anion is only half the size in [(P)Fe(C_6H_5)(py)]$^-$, as compared to the five-coordinate species generated in PhCN (see Table III). This suggests a weaker contribution of the iron(III) radical anion form to the reduction process (eq 11) and implies a smaller overlap of the d_{xz} and d_{yz} HOMOS of the iron with the e_g LUMO of the porphyrin, presumably resulting from a greater separation of their respective energy levels. This phenomenon is not surprising, since ^{1}H NMR measurements clearly indicate a marked back-bonding effect induced upon coordination of the iron ion by pyridine.

The back-bonding ability of the pyridine ligand is weak enough to place the d_{xz} and d_{yz} orbital energy levels at almost the same distance from the e_g LUMO and the a_u

(26) Lau, W.; Huffman, J. C.; Kochi, J. K. *Organometallics* **1982**, *1*, 155.

HOMO energy levels of the porphyrin. This is evidenced by the oxidation pattern of (OEP)Fe(C_6H_5)(py) that, as indicated by time-resolved electronic absorption spectra, involves both spin-coupled iron(III) radical cation and iron(IV) porphyrin cation forms.

In summary we have shown that pyridine coordinates to oxidized, neutral, and reduced iron(III)–phenyl σ-bonded five-coordinate porphyrins producing the corresponding six-coordinate derivatives. This coordination results in stabilization of the neutral and oxidized species. Also we report the first case where oxidation and reduction of the same iron(III) porphyrin can be described as occurring at a location involving both the central metal orbitals and those of the π ring system. These electrochemical reactions can be described by a mixed formalism involving an Fe(IV) complex and an Fe(III) cation radical, as well as an Fe(II) complex and an Fe(III) anion radical.

Acknowledgment. The support of the National Institutes of Health (GM 25172) is gratefully acknowledged.

Registry No. (OEP)Fe(C_6H_5)(py), 90148-87-1; (TPP)Fe(C_6H_5)(py), 90148-88-2; (OEP)Fe(C_6H_5), 83614-06-6; (TPP)Fe(C_6H_5), 70936-44-6; [(OEP)Fe(C_6H_5)(py)]$^+$, 90148-89-3; [(TPP)Fe(C_6H_5)(py)]$^-$, 90148-90-6.

Bridged Ferrocenes. 10.[1] Structural Phenomena

Manny Hillman,* Etsuko Fujita, and Helen Dauplaise

Chemical Science Division, Department of Applied Science, Brookhaven National Laboratory, Upton, New York 11973

Åke Kvick

Department of Chemistry, Brookhaven National Laboratory, Upton, New York 11973

Robert C. Kerber

Department of Chemistry, State University of New York at Stony Brook, Stony Brook, New York 11797

Received February 21, 1984

The structures of 1,1′,2,2′-bis(tetramethylene)ferrocene, I, 1,1′,2,2′,4,4′-tris(tetramethylene)ferrocene, II, and 1,1′,2,2′,4,4′-tris(pentamethylene)ferrocene, III, are given and are compared to the previously determined[2] structure of 1,1′,2,2′,4,4′-tris(trimethylene)ferrocene, IV. The iron-to-ring distances are consistent with the reported Mössbauer spectra[3] and redox potentials.[4] The cyclopentadienyl rings are eclipsed in the compounds with trimethylene and pentamethylene bridges but are staggered by 12–14° in the compounds with tetramethylene bridges. In compounds with tetra- and pentamethylene bridges the presence of staggering or eclipsing is attributed to the need to avoid eclipsing of the protons in the bridges. In the compound with three trimethylene bridges, the shortness of the bridges is of primary importance. The staggered conformation observed in I and II may be the source of the apparent anomalies observed in the ring-proton region of the NMR spectra of bridged ferrocenes. The bridge-proton region of the NMR spectra at 360 MHz are given for I and other bridged ferrocenes. Disorder of the bridge carbons observed in the crystals are correlated with the flipping of the bridges observed in the NMR spectra.

Introduction

In the NMR spectra reported for the bridged ferrocenes,[5] anomalies occur. The separation of the chemical shifts of the ring protons is greater in ferrocene with a trimethylene bridge ($\Delta\delta$ = 0.05 ppm) than in ferrocene with a tetramethylene bridge ($\Delta\delta$ = 0.04 ppm). This is in accord with the observation[6-8] that greater ring tilting leads to a greater separation of the chemical shifts of the ring protons. However, in ferrocene with a pentamethylene bridge the separation of the chemical shifts of the ring protons ($\Delta\delta$ = 0.11 ppm) is greater than even in trimethyleneferrocene. Similar reversals have been reported[5] for the related compounds with two and three bridges. E.g., the ratios of the ring-proton peaks (downfield to upfield) are 2:1, 1:2, and 2:1 for V, VI, and VII (all structures are illustrated in Figures 1–5), respectively. It was anticipated that some variance in the structures of the tetramethylene and pentamethylene derivatives was responsible for these anomalies. For this reason an attempt is underway to determine the structures of relevant bridged ferrocenes. In this paper the structures of a bis(tetramethylene)-, I, a tris(tetramethylene)-, II, and a tris(pentamethylene)-ferrocene, III, are reported.

Experimental Section

Compounds I, II and III were prepared by the procedures of Hisatome et al.[5,9,10] Crystals were grown from hexane solutions and were mounted along their long axes for the collection of the diffraction intensity data.

The intensity data were collected on an Enraf-Nonius CAD-4 diffractometer with graphite-monochromated Mo Kα radiation (λ = 71.07 pm). The crystal data are given in Table I. The

(1) Paper 9 of series: Hillman, M.; Matyevich, L.; Fujita, E.; Jagwani, U.; McGowan, J. *Organometallics* **1982**, *1*, 1226–9.
(2) Hillman, M.; Fujita, E. *J. Organomet. Chem.* **1978**, *155*, 87–98.
(3) Hillman, M.; Nagy, A. G. *J. Organomet. Chem.* **1980**, *184*, 434–445.
(4) Fujita, E.; Gordon, B.; Hillman, M.; Nagy, A. G. *J. Organomet. Chem.* **1981**, *218*, 105–114.
(5) Hisatome, M.; Hillman, M. *J. Organomet. Chem.* **1981**, *212*, 217–231.
(6) Rinehart, K. L., Jr.; Frerichs, A. K.; Kittle, P. A.; Westman, L. F.; Gustafson, D. H.; Pruett, R. L.; McMahon, J. E. *J. Am. Chem. Soc.* **1960**, *82*, 4111–4112.
(7) Barr, T. H.; Watts, W. E. *Tetrahedron* **1968**, *24*, 6111–6118.
(8) Hillman, M.; Weiss, A. J. *J. Organomet. Chem.* **1972**, *42*, 123–128.
(9) Hisatome, M.; Sakamoto, T.; Yamakawa, K. *J. Organomet. Chem.* **1976**, *107*, 87–101.
(10) Hisatome, M.; Watanabe, N.; Sakamoto, T. Yamakawa, K. *J. Organomet. Chem.* **1977**, *125*, 79–93.

0276-7333/84/2303-1170$01.50/0